Journal Pre-proof

A novel biosensor for zinc detection based on microbial fuel cell system

Aman Khan, El-Sayed Salama, Zhengjun Chen, Hongyuhang Ni, Shuai Zhao, Tuoyu Zhou, Yaxin Pei, Rajesh K. Sani, Zhenmin Ling, Pu Liu, Xiangkai Li

Please cite this article as: Khan, A., Salama, E.-S., Chen, Z., Ni, H., Zhao, S., Zhou, T., Pei, Y., Sani, R.K., Ling, Z., Liu, P., Li, X., A novel biosensor for zinc detection based on microbial fuel cell system, *Biosensors and Bioelectronics* (2019), doi: https://doi.org/10.1016/j.bios.2019.111763.

This is a PDF file of an article that has undergone enhancements after acceptance, such as the addition of a cover page and metadata, and formatting for readability, but it is not yet the definitive version of record. This version will undergo additional copyediting, typesetting and review before it is published in its final form, but we are providing this version to give early visibility of the article. Please note that, during the production process, errors may be discovered which could affect the content, and all legal disclaimers that apply to the journal pertain.

1   **A novel biosensor for zinc detection based on microbial fuel cell system**

2   Aman Khan[a,1], El-Sayed Salama[b,c,1], Zhengjun Chen[d], Hongyuhang Ni[a], Shuai Zhao[a], Tuoyu
3   Zhou[a], Yaxin Pei[a], Rajesh K Sani[e], Zhenmin Ling[a], Pu Liu[a,f], Xiangkai Li[a,f]*

4

5   [a]*MOE, Key Laboratory of Cell Activities and Stress Adaptations, School of Life Science,*
6   *Lanzhou University, Lanzhou, 730000, Gansu, PR China*
7   [b]*Department of Occupational and Environmental Health, School of Public Health, Lanzhou*
8   *University, Lanzhou 730000, Gansu, PR China*
9   [c]*Department of Earth Resources and Environmental Engineering, Hanyang University, Seoul*
10   *04763, South Korea*
11   [d]*College of Life Science and Technology, Gansu Agricultural University, Lanzhou 730070,*
12   [e]*Department of Chemical and Biological Engineering South Dakota School of Mines and*
13   *Technology, 501 East St. Joseph Street Rapid City, SD, USA. 57701-3995*
14   [f]*Key Laboratory for Resources Utilization Technology of Unconventional Water of Gansu*
15   *province, Gansu Academy of Membrane Science and Technology, Lanzhou 730020, Gansu, PR*
16   *China*

17

18

19

20

21

22   *Corresponding Author
23   E-mail: xkli@lzu.edu.cn
24   Tel: 86-0931-8912561
25   [1]These authors contributed equally to this work.

26

27 **Abstract**

28   Microbial fuel cell (MFC) biosensors are self-sustainable device for monitoring of

29 various substrates; however, for heavy metals detection are still scarce. In this study, *E. coli*

30 BL21 was engineered to express the *znt*R, *rib*B, and *opr*F genes with P_{zntA} promoter, which

31 could sense zinc (Zn^{2+}) for riboflavin and porin production. The engineered strain produced high

32 levels of riboflavin (2.4-3.6 µM) and improved cell membrane permeability, with a positive

33 correlation of Zn^{2+} (0-400 µM). The strain was then employed in MFC biosensor under the

34 following operational parameters: external resistance 1000 Ω, pH 9, and temperature 37 °C for

35 Zn^{2+} sensing. The maximum voltages (160, 183, 260, 292, and 342 mV) of the constructed MFC

36 biosensor have a linear relationship with Zn^{2+} concentrations (0, 100, 200, 300, and 400 µM,

37 respectively) (R^2 = 0.9777). An Android App was developed for the biosensor system that could

38 sense Zn^{2+} in real-time and *in situ*. The biosensor was applied to wastewater with different Zn^{2+}

39 concentrations and the results showed that the detection range for Zn^{2+} was 20-100 µM, which

40 covers common Zn^{2+} safety standards. The results obtained with developed MFC biosensor were

41 comparable to conventional methods such as colorimetric, flame atomic absorption spectroscopy

42 (FAAS), and inductively coupled plasma optical emission spectroscopy (ICP-OES). In summary,

43 MFC biosensor with biosynthetic strain is an efficient and affordable system for real-time

44 monitoring and sensing of heavy metals.

45

46 **Keyword:** MFC; Zn^{2+} biosensor; Cell permeability; Electron shuttle mediator

47

1. Introduction

48

49   Zinc is an abundant transitional metal that serves catalytic, structural, redox-modulatory,

50   and regulatory roles owing to its high binding affinity, which is next to that of copper among the

51   Irving-Williams series of metals (Choi et al., 2017). Long term exposure and high dose of Zn^{2+}

52   supplementation and accumulation can cause significant toxicity and is shown to affect digestive

53   and respiratory tracts (Poddalgoda et al., 2019). Therefore, detection of Zn^{2+} in water samples is

54   important for zinc contamination control. The determination of metal concentrations in water by

55   conventional methods such as gas chromatography-mass spectroscopy (GC-MS) (Takeuchi et al.,

56   2019), flame atomic absorption spectroscopy (FAAS) and inductively coupled plasma optical

57   emission spectroscopy (ICP-OES) (Escudero et al., 2010), and inductively coupled plasma-mass

58   spectrometry (ICP-MS) (Ravikumar et al., 2012) have been performed successfully. Despite

59   these analytical methods are expensive, energy-consuming, require pretreated samples (Li et al.,

60   2015), and may not be accessible to rural areas in developing countries (Bereza-Malcolm et al.,

61   2015). A cost-effective and self-sustaining technique needs to be developed for the assessment of

62   metal toxicity in water samples.

63   A bacterial biosensor is an alternative to analytical methods with reduced cost and labor

64   for detection of metals based on fluorescence proteins or pigment molecules connected to metals

65   sensing operons (regulator) (Cerminati et al., 2015; Choi et al., 2017). Several biosensors have

66   been designed and constructed by employing synthetic biology tools for heavy metals (HMs)

67   detection (Kim et al., 2016; Rijavec et al., 2016). Zn^{2+} metal ions are sensed by the zinc regulator

68   ZntR of the MerR and CzrA/SmtB/AztR/ArsR family (Choi et al., 2017; Webster et al., 2014). *E.*

69   *coli* MC1061 (p*zntRluc*) biosensor detected 2% Zn^{2+} metal ion of the total amount in soil-water

70   extracts (Ivask et al., 2002). *Synechocystis* sp. PCC6803 (p*coaTlux*) monitored 90 % of Zn^{2+}

71   along with Ni^{2+} and Co^{2+} HMs in the soil mixture contaminated with various chemicals and oily

72 wastes (Peca et al., 2008). Detection of Zn^{2+} based on a reporter gene system is of poor

73 sensitivity and not specific (Liu et al., 2012). This system needs an additional signal transducer

74 or external power source with limited detection efficiency (Tanikkul and Pisutpaisal, 2018).

75 Hence, there is a growing demand to develop a system for *in situ* real-time monitoring of HMs

76 toxicity in water.

77   Microbial fuel cell (MFC) based biosensors are widely used to monitor a broad spectrum

78 of environmental parameters such as biological oxygen demand (Yu et al., 2013), chemical

79 oxygen demand (Su et al., 2011), and organic substrates toxicity (Chen et al., 2016; Kim et al.,

80 2007) in wastewaters. The MFC-based sensor is an advanced system that develops a linear

81 relationship between substrate concentrations and voltages by improving the selectivity and

82 sensitivity of toxicity detection (Yi et al., 2018). Electrons shuttle mediator (riboflavin)

83 facilitated transfer of electrons to increase voltage in MFC (Li et al., 2018; Yang et al., 2015).

84 Flavin biosynthesis genes cluster *rib*ABCDEHC could synthesize riboflavin and improve MFC

85 performance through the extracellular electron transfer (EET) mechanism (Tao et al., 2015; Yang

86 et al., 2015). However, low membrane permeability of cells of bacterial strains restricted the

87 transfer of electrons from the cells to the electrodes (Liu et al., 2014). *E. coli* has a compact and

88 less permeable outer membrane (OM) with limited electron transfer (Muheim et al., 2017).

89 Overexpression of *opr*F in *E. coli* BL21 enhanced OM permeability and allowed more electrons

90 to get transferred from the OM to the inner membrane and then to the electrode (Yong et al.,

91 2013b).

92   The present study was conducted to develop a novel, genetically engineered, Zn^{2+}-

93 specific MFC biosensor with *E. coli* BL21 that carried the *rib*B (biosynthetic enzyme 3, 4-

94 dihydroxy-2-butanone-4-phosphate synthase) cognate with P_{zntA} promoter and *opr*F (porin

4

95   synthetic protein) genes. The constructed biosensor was calibrated for specific operational

96   parameters such as sensitivity, specificity, and stability. The engineered BL21 strain was also

97   investigated for cell membrane permeability and riboflavin synthesis in the MFC. A linear

98   relationship was developed between Zn^{2+} concentrations and electric signals using the engineered

99   BL21 strain as a biosensor in the MFC. Furthermore, the constructed MFC biosensor was

100   compared with conventional methods such as colorimetric, FAAS, and ICP-OES with respect to

101   the detection of Zn^{2+} in wastewater. The constructed MFC biosensor would be a suitable device

102   for real-time monitoring and sensing of HMs in wastewater with a direct electrical output.

103   **2. Materials and Methods**

104   *2.1. In vitro gene synthesis and plasmid construction*

105   Molecular biological tools were used to construct the plasmids pUC19 and pETDuet-1.

106   The zinc-responsive regulator/promoter (p*znt*R) and riboflavin synthetic (*rib*B) genes were

107   amplified from the genome of *Shewanella oneidensis* MR-1 and porin protein (*opr*F) gene was

108   amplified from *Pseudomonas aeruginosa* using a set of primers with restriction sites. The green

109   fluorescent protein (GFP) gene was present in our laboratory stocks. *znt*R was overlapped with

110   *gfp* and the fragment was digested with *Hind*III and *Bam*HI and inserted into the plasmid pUC19

111   under the control of the P_{zntA} promoter. The recombinant plasmid was named pUC19-pzntR-GFP

112   and transferred into *E. coli* W-1 for expression. To avoid the high error rate of a long fragment

113   building block, we overlapped the p*znt*R and *rib*B and the resultant fragment was digested with

114   *Bam*HI and *Eco*R1. The digested fragment was ligated downstream of the *opr*F gene under the

115   control of Zn^{2+} inducible promoter P_{zntA}. The resultant plasmid was named pETDuet-1pzntR-

116   ribB-oprF and was transferred into the host strain *E. coli* BL21 (DE3) for expression (Table 1).

117   All gene coding sequences and information were obtained from the NCBI, BioCyc database and

118　screened using PCR. The engineered BL21 strain was cultured in LB medium or M9 medium

119　(1× M9 medium, 2 mM/L MgSO$_4$, 0.1 mM/L CaCl$_2$, and 0.4% glucose as a carbon source) at 37

120　°C with shaking at 180 rpm. Ampicillin (50 μg/mL) and IPTG (0.7 mM) were added to the

121　culture medium whenever needed. Engineered cells (1 mL) were grown in 100 mL LB-broth and

122　the culture was incubated at 37 °C in a shaking incubator until OD$_{600}$ reached 0.6.

Table 1

Oligonucleotide primers, plasmids, and bacterial strains used in this study.

Primers name	Sequence	PCR product
ZntR-F	CGCGGATCCATGTATCGCATTGGTGAGCTG	
ZntR-R	CCGGAATTCACAACCACTCTTAACGCCACTC	p*znt*R-operon
Rib-F	CCCTCGAGGGATGAATCAGACGCTACTTTCCTC	
Rib-R	ATTTGCGGCCGCGCTGGCTTTACGCTCATGTG	*rib*B-operon
OprF-F	CGCGGATCCATGAAACTGAAGAACACCTTAGGC	
OprF-R	CCGGAATTCCAACCGATTTCCCTGAGCG	*opr*F-operon
GFP-F	CGCGGATCCATGAGTAAAGGAGAAGAACTTTTCA	
GFP-R	CCCTCGAGTTTGTATAGTTCATCCATGCCATGT	*gfp*-operon
ZntRrib-F	TTAAGATTGTTGCGCAGGAGATATCGCATTGGTGAGCTGGCAAAAA	
ZntRrib-R	TGCCAGCTCACCAATGCGATATCTCCTGCGCAACAATCTTAACGCAT	p*znt*R-*rib*B-operon
ZntRGFP-F	TGGCGTTAAGAGTGGTTGTATGAGTAAAGGAGAAGAAC	
ZntRGFP-R	AGTTCTTCTCCTTTACTCATACAACCACTCTTAACGCCAC	p*znt*R-*gfp*-operon
QpzntR-F	AAGGCATTGTGCAGGAAAGA	
QpzntR-R	CCACAACAGGCATCGTTAAG	

Plasmids and strains	Relevant characteristic	Source
pUC19	Clone vector, Amp^R	Laboratory
pET-Duet-1	Clone and expression vector, Amp^R,	Laboratory
pUC19-pzntR-GFP	Recombinant plasmid containing pzntR and GFP	This study
pETDuet-1pzntR-ribB-oprF	Recombinant plasmid containing p*znt*R, *rib*B, and *opr*F genes	This study
S. oneidensis MR-1	Containing p*znt*R and *rib*B genes	Laboratory
P. aerogenosa	Containing *opr*F gene	Laboratory
E. coli DH5α	Clone host strain, containing recombinant plasmid pUC19-pzntR-GFP	This study
E. coli BL21 (DE3)	Expression strain, containing recombinant plasmid pETDuet-1pzntR-ribB-oprF	This study

7

123   *2.2. Real-time PCR, flow cytometry, and fluorescence microscopy*

124   The expression of pUC19-pzntR-GFP was measured using RT-PCR. The engineered and

125   wild type (WT) *E. coli* W-1 strains were grown in LB-broth at 37 °C to an OD_{600} of 0.6, and

126   different concentrations (0, 30, 60, and 90 μM) of Zn^{2+} were added individually. After 3 h of

127   Zn^{2+} addition, cells were harvested and total RNAs were isolated using the SV total RNA

128   isolation kit (Promega). Quantitative RT-PCR reactions were performed under the following

129   conditions: cDNA synthesis (50 °C, 40 min), denaturation (95 °C, 12 min), and amplification for

130   40 cycles (95 °C, 20 sec; 60 °C, 1 min). A flow cytometry test was applied, *E. coli* W-1 cells

131   carrying pUC19-pzntR-GFP were cultured with $ZnCl_2$, $NiCl_2$, $CuCl_2$, $HgCl_2$, $CoCl_2$, and

132     $Pb(NO_3)_2$ (final concentration, 90 μM). *E. coli* DH5α containing the empty plasmid was used as

133   a control. A flow cytometer (BD LSRFortessa, USA) equipped with a 488 nm blue solid-state

134   laser was used to observe the cell population at a flow rate of 1 μL/s. For fluorescence

135   microscopy, the engineered cells were induced with Zn^{2+} and harvested after 4 h of

136   centrifugation (3500 × *g* for 5 min) at 4 °C. The cells were washed with phosphate-buffered

137   saline (PBS) solution and re-suspended in PBS solution supplemented with 0.3% agarose. A

138   fluorescence microscope (Olympus, Japan) with a cooled charge-coupled device camera (B&W

139   SenSys, KAF1401) was used to screen the cells.

140   *2.3. Membrane permeability assay*

141   The membrane permeability of the engineered strain BL21 carrying the recombinant

142   plasmid, pETDuet-1pzntR-ribB-oprF was assessed by o-nitrophenyl-b-galactopyranoside

143   (ONPG) hydrolysis (Arcidiacono et al., 2009). The overnight culture of the engineered

144   BL21strain was inoculated in fresh LB medium. After 5 h of incubation at 37 °C, cells were

145   harvested and washed thrice with PBS buffer (10 mM, pH 7.4). The ONPG hydrolysis assay was

146 performed by mixing 135 mL of ONPG solution (1.5 mM in 10 mM PBS, pH 7.4) with 15 mL of

147 cells suspension. The absorbance of the mixture was measured at 405 nm on a microplate reader

148 (Thermo Scientific, MA, USA). The WT BL21 strain was used as a control and the assay was

149 performed in triplicate.

150 *2.4. MFC design and biosensor operation*

151 A two-chambered MFC operating reactor was set up, each bottle with a working volume

152 of 240 mL divided by proton exchange membrane (PEM; Naf on117, DuPont, USA). The PEM

153 and electrodes were pretreated before use (Chen et al., 2016). Carbon felt as electrodes with an

154 area of 16 cm^2 geometric surfaces were used as anode and cathode. The electrodes were linked

155 with a 1000 Ω external resistor *via* titanium wire. During the MFC operating system, the anode

156 medium was M9 supplemented with the different concentrations (0–400 μM) of Zn^{2+} metal in

157 the interest of the Zn^{2+} responsive regulator. The catholyte was potassium ferricyanide (100 mM

158 potassium ferricyanide in 50 mM phosphate buffer, pH 7.0). The MFC reactor was operated at

159 37 °C and 180 rpm using a magnetic stirrer. A data acquisition apparatus was used to record the

160 voltage at 10 min intervals in the MFC biosensor. Furthermore, Zn^{2+} concentrations from 0 to

161 500 μM were also examined in the MFC in different batches. The anode medium was refreshed

162 after 15 h of incubation and the concentration was changed for each batch. The Zn^{2+}

163 concentrations were increased gradually in each batch of operation in the same MFC.

164 A portable biosensor was developed where the sensor was able to collect voltage signals

165 through a data acquisition card, convert them into digital signals, record, and display real-time

166 signals using Android system App. The software was developed in Android studio with Java

167 language. The collected experimental data was run on the App, which displayed it in the real-

168 time in the form of dynamic graphs. The App was modified form our previous *p*-nitrophenol

169 software (Chen et al., 2016). The signal acquisition software can also calculate the relationship

170 between voltage and Zn^{2+} ions. The developed software has been uploaded to GitHub

171 (https://github.com/maomao0601/CollectingData) (Supplementary materials).

2.5. Optimization parameters for the biosensor test

173   The constructed sensor strain BL21 was applied in MFC to optimized parameters for

174 working condition. The engineered BL21 strain was grown in different Zn^{2+} concentrations (0–

175 800 µM), temperatures (25, 30, 37, and 45 °C), pH values (5.5, 7.01, 8.02, 9.00, and 11.00), and

176 heavy metals including $ZnCl_2$, $NiCl_2$, $CuCl_2$, $HgCl_2$, $CoCl_2$, and $Pb(NO_3)_2$ at a final concentration

177 of 300 µM supplemented with the M9 medium in the MFC reactor. All experiments were

178 performed in triplicate.

2.6. Application of the constructed MFC biosensor in wastewater

180   The engineered BL21 sensor strain was applied for practical application in synthetic

181 wastewater. A dual-chambered MFC device (working volume of 240 mL) with synthetic

182 wastewater and M9 fresh medium (1:1) supplemented with 0, 20, 60, and 100 µM of Zn^{2+}

183 concentrations were set up (Cerminati et al., 2015). The concentration was selected based on

184 common Zn^{2+} levels observed in the M9 growth media. Increase in voltage defined the exposure

185 of Zn^{2+} at different concentrations and detection of Zn^{2+} in the MFC reactor was measured by

186 electric signals. The same Zn^{2+} contaminated water was also measured using analytical methods

187 such as colorimetric, FAAS, and ICP-OES and the results were compared with those of the MFC

188 biosensor.

2.7. Analytical methods

190   Voltage was calculated according to $I = V/R$ (Ohm's law), where I is the current, V is the

191 observed voltage, and R, external resistance, and $P = VI$, where P is power. The anode geometric

10

192 surface area (16 cm^2) was used for current density (mA m^{-2}) and power density (mW m^{-2})

193 calculations. Open-circuit voltage (OCV) was maximum voltage where the external resistance is

194 infinite. The external resistance declining from 9999 to 100 Ω was used to determine the

195 polarization curve (Logan, 2009). Riboflavin concentration in the anode electrolyte of the MFC

196 was examined by time course induction using HPLC equipped with a UV detector. The column

197 used was an Agilent analytical C18 (4.6 mm × 105 mm) (Agilent, USA). In detail, 2 mL of the

198 electrolyte samples were collected at 12 h intervals from the MFC reactor and centrifuged (6000

199 rpm, 5 min). For HPLC analysis, the supernatant was filtrated with a 0.22 μm cellulose

200 membrane and subjected to the system according to the procedure described by Vasilaki et al.

201 (2010). The supernatant (10 μL) was then analyzed with an eluent of 50% methanol and 50%

202 ddH$_2$O at 1.0 mL/min of flow rate and the HPLC profile was observed at 270 nm.

203 Cyclic voltammetry (CV) was implemented in a three-electrode configuration with an

204 Ag/AgCl reference electrode with a potentiostat (CHI604E, Shanghai, China). The CV scan rate

205 was 5 mV/s in the range from -0.8–0.8 V (vs SHE). A scanning electron microscope (s-3400,

206 HITACHI, Japan) was used to observe the formation of anode biofilms on an electrode. The

207 experimental data in triplicate was statistically analyzed using mean and standard deviations. All

208 graphs and curve fits were prepared in GraphPad Prism 7 (GraphPad, San Diego, CA, USA) and

209 Origin 8.0 (Origin Lab, Massachusetts, and USA).

3. Results and discussion

3.1. Construction of Zn^{2+} detecting exoelectrogen

212 To construct the *E. coli* strain that can sense Zn^{2+} and generate electricity, *znt*R, *rib*B,

213 *opr*F, and cognate promoter P$_{zntA}$ were cloned into pUC19 and pETDuet-1 (Fig. 1a). A

214 constructed plasmid named pUC19-pzntR-GFP containing a transcriptionally insulated p*znt*R

215   controlling the expression of GFP. RT-PCR results revealed that the transcription level of the

216   zinc-responsive regulator/promoter was increased to a maximum of 8.5-folds at 90 µM

217   concentration of Zn^{2+} (Fig. 1b). Under the supplementation of different metals ions, the flow

218   cytometry results showed that the constructed Zn^{2+} sensor was highly responsive to Zn^{2+} ion and

219   not sensitive to other divalent metals, such as Cu^{2+}, Ni^{2+}, Pb^{2+}, Hg^{2+}, and Co^{2+} (Fig. 1c). Data

220   from fluorescence microscopy showed that the Zn^{2+} inducible promoter up-regulated

221   downstream genes and synthesize green fluorescence protein (Fig. 1d). This data confirmed that

222   Zn^{2+} metal induces pzntR expression. Then, the GFP gene was replaced by *rib*B and cloned

223   along with *opr*F into the pETDuet-1 plasmid. The recombinant plasmid was transferred to the *E.*

224   *coli* BL21 for expression. The transformant showed that the *opr*F expression in the engineered

225   strain BL21 increased the cell membrane permeability, which was 4.5 times higher than that of

226   the WT BL21 strain (control) carrying the vacant plasmid (Fig. 1e).

227   Metal-responsive regulatory units originating from bacterial species have been used in

228   metal biosensors such as MerR or ArsR/SmtB-like regulators (Cerminati et al., 2011; Webster et

229   al., 2014). A whole-cell Zn^{2+}-specific bacterial biosensor has been developed for monitoring of

230   Zn^{2+} ions in human serum showed that the p*znt*A regulator/promoter was up-regulated at a lower

231   range of 20 µM of Zn^{2+} (Watstein and Styczynski, 2018). p*zit*B is a Zn^{2+} responsive

232   regulator/promoter and the relative expression was 5.6-fold at 100 µM of Zn^{2+} (Choi et al.,

233   2017), which was consistent with the present study that showed 8.5-folds transcriptional level of

234   p*znt*R at 90 µM of Zn^{2+}. Transfer of electrons *via* the OM of electrochemically active bacteria to

235   the electrode was restricted due to the dense and strong layer of lipopolysaccharide on the

236   surface cover (Wen et al., 2011; Yong et al., 2014). Overexpression of *opr*F enhanced 4.5 times

237   OM permeability of engineered strain (Fig.1e).
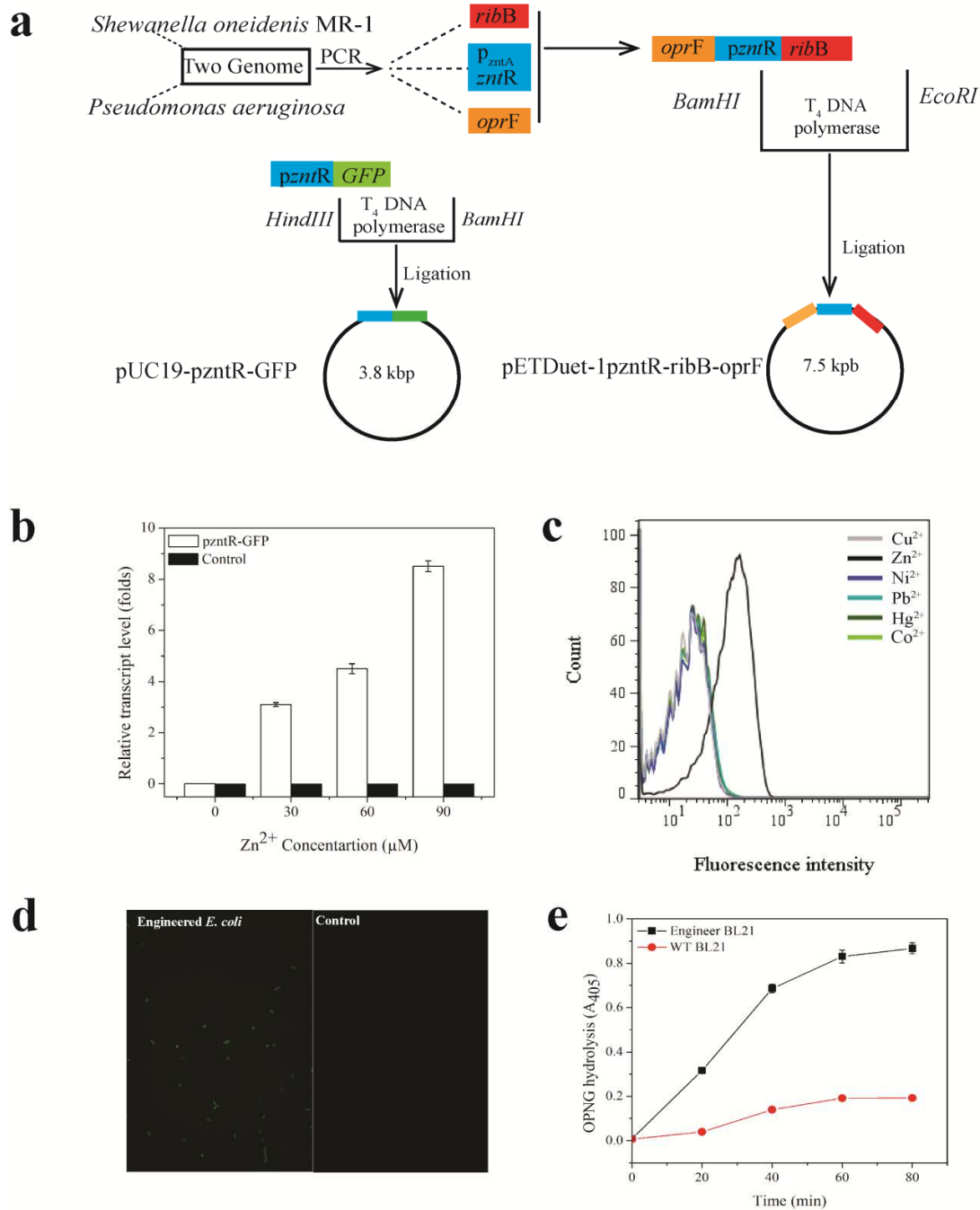
Fig. 1. (**a**) Flowchart of constructed co-expression vector pUC19 and pETDuet-1, (**b**) RT-PCR by using Zn^{2+} concentrations (0, 30, 60, 90 µM), (**c**) Flow cytometry of different metal ions (Cu^{2+}, Zn^{2+}, Ni^{2+}, Pb^{2+}, Hg^{2+} and Co^{2+}) at 90 µM of final concentration, (**d**) Fluorescence microscopy profiles of *E.coli* W-1 carrying the recombinant plasmid pUC19-pzntR-GFP and control, and (**e**) Cell permeability of engineered strain BL21 carried recombinant plasmid pETDuet-1pzntR-ribB-oprF.

238 The obtained results were accordingly to Yong et al. (2013b) by expressing *opr*F in *E. coli* BL21

239 which increased OM permeability 3.2 times as compared to that by the control strain. These data

240 indicated that p*znt*R, *rib*B, and *opr*F were successfully over-expressed and facilitated the

241 movement of inward electrons outward during EET mechanism in constructed Zn^{2+} specific

242 sensor.

243 *3.2. Linear relationship between Zn^{2+} concentrations and voltage generation*

244   The constructed Zn^{2+} sensing strain was applied in a two-chambered MFC with different

245 concentrations of Zn^{2+} and the voltage output was monitored. The maximum voltage generation

246 (160, 183, 260, 292, and 342 mV) was correlated with the Zn^{2+} concentrations (0, 100, 200, 300,

247 and 400 µM, respectively) (Fig.2a). A significant linear relationship between Zn^{2+} concentrations

248 and the maximum voltage of the constructed MFC biosensor was observed ($R^2 = 0.9777$) (Fig.

249 2b). Moreover, the amendment of Zn^{2+} concentrations at different batches led to an increase in

250 voltage generation from 98 mV to 189 mV at 0–400 µM using the engineered BL21 strain (Fig.

251 2c). Increasing Zn^{2+} concentration to 500 µM inhibited the voltage generation. Riboflavin is a

252 key factor in promoting MFC voltage generation. Maximum riboflavin production in the anolyte

253 was observed from 2.41 µM/L to 3.6 µM/L at 100–400 µM of Zn^{2+} concentrations within 120 h

254 of incubation, while there was no flavin production observed at 0 concentration of Zn^{2+} (Fig. 2d).

255 The results suggested that the *rib*B gene induces by Zn^{2+} responsive promoter and elevated the

256 voltage generation in MFC. This data indicated that the constructed MFC biosensor enabled the

257 cell to respond to Zn^{2+} in a dose-dependent manner and synthesize flavins in the MFC.

258   Zn^{2+} specific biosensor *P. putida* X4 (pczcR3GFP) was fabricated by fusing *egfp* with

259 *czc*R3 promoter which showed a relative relationship between Zn^{2+} concentrations and

260 fluorescence intensity in a range (5–55 µmole/L) of Zn^{2+} in soil extract (Liu et al., 2012). The

14

261 correlation between Zn^{2+} concentrations (100–1000 µM) and relative fluorescence was found

262 linear by employing *E. coli* carried *zra*P and GFP in LB media (Ravikumar et al., 2011). Zn^{2+}

263 sensor based on pigment molecule response responded to Zn^{2+} in the range of 10, 20, and 100

264 µM in human serum (Watstein and Styczynski, 2018). Detection of Zn^{2+} by fluorescence

265 measurement is not suitable for real-time monitoring; however, this drawback was overcome

266 using the MFC-based biosensor. An arsenic (p*ars*R) specific biosensor constructed in *S.*

267 *onidensis* MR-1 strain showed a linear relationship at 0–100 µM of arsenic concentrations with

268 the maximum current peak ranging from 10 µA to 40 µA in the bioelectrochemical system

269 (Webster et al., 2014). This was consistent with the present study where a correlation curve was

270 observed between Zn^{2+} concentrations and voltages $R^2 = 0.9777$. Detection of benzoylecgonine

271 in urine-based wastewater examined in batch MFC showed that increasing concentrations of

272 benzoylecgonine (0–3.45 µM) led to decline the voltage from 0.31 V to 0.26 V (Catal et al.,

273 2019). In contrast, detection of Zn^{2+} in batch MFC was associated with electricity generation

274 assisted by riboflavin production. The genes cluster, *rib*ABCDE inserted in *E. coli* BL21 can

275 increase voltage by 9.6-fold than that present in the control by producing riboflavin in anode

276 MFC (Tao et al., 2015). *S. oneidensis* carrying *rib*ADEHC genes cluster could synthesize 25.7

277 µM/L of riboflavin and produce 13.2-fold of voltage (Yang et al., 2015). The results indicated

278 that the voltage alteration was directly related to the quantity of Zn^{2+} in the medium that showed

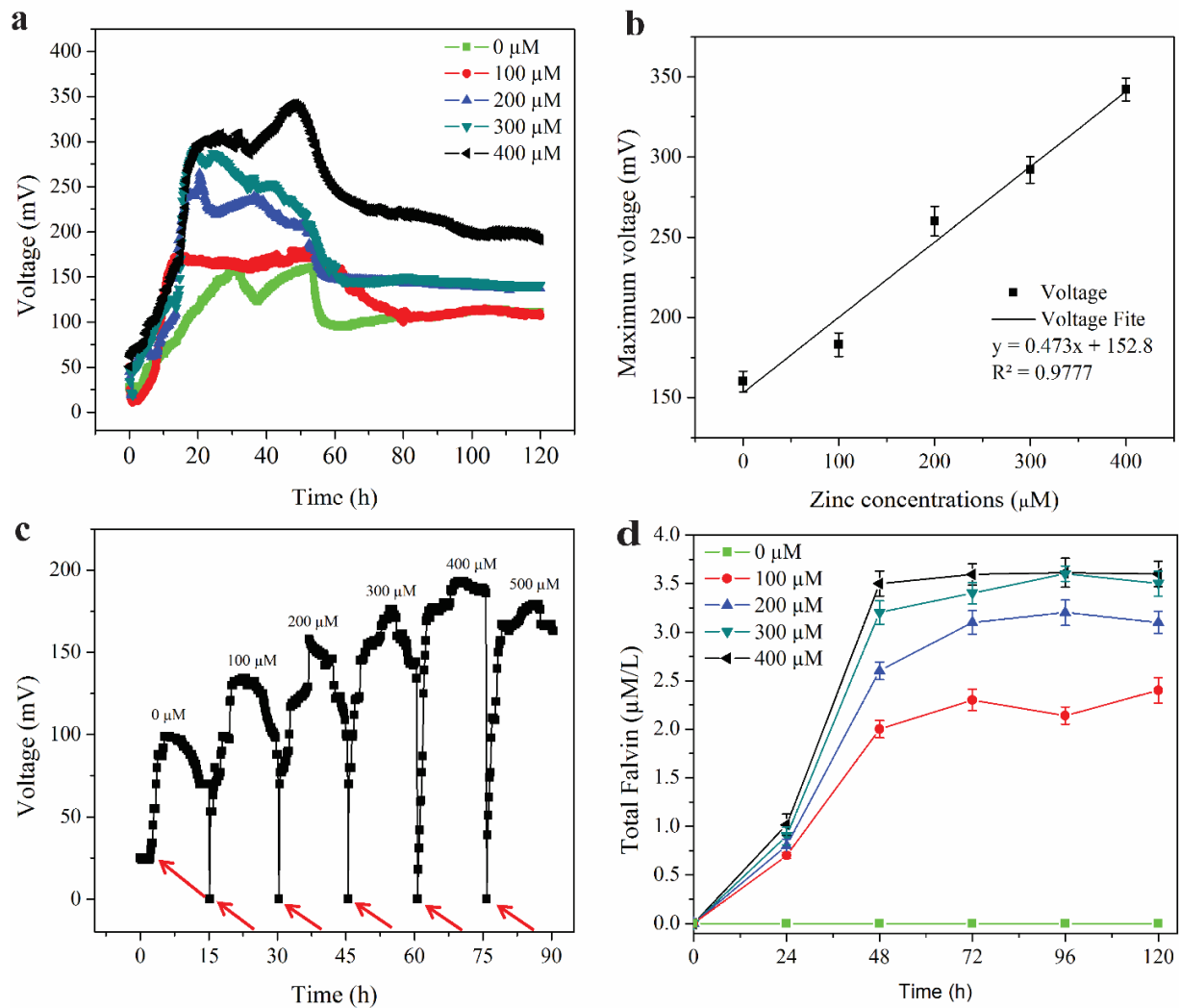279 the bio-sensing capability and sensitivity of the engineered BL21 strain.

Fig. 2. (a) Voltage generation by engineered BL21 strain at different concentrations of Zn^{2+} from 0 to 400 µM, **(b)** A linear relationship curve between the maximum voltage and Zn^{2+} concentrations, **(c)** riboflavin production at a different time interval**, (d)** biofilm-based MFC in different batches. Arrows indicate the addition of fresh medium.

3.3. *Influence of different environmental parameters on constructed Zn^{2+} sensor in MFC*

The constructed sensor strain was applied for practical applications under the various environmental parameters for optimization in MFC. The results revealed that the maximum voltage was generated by the MFC biosensor enhanced from 158 mV to 341 mV at 0 to 400 µM of Zn^{2+} concentrations (Fig. 3a) and showed a linear relationship (R^2=0.9882) among these parameters (Fig. 3b). Electricity generation decreased from 341 mV to 240 mV at 600 and 800

16

286 µM of Zn^{2+}. This indicated that voltage established a linear relationship with Zn^{2+} concentrations

287 which ensures the sensitivity and selectivity of the constructed MFC biosensor. It was also

288 observed that a temperature of 37 °C is suitable for the growth of the engineered BL21 strain

289 (Fig. 3c). When the temperature increased to 45 °C, voltage output significantly reduced because

290 of the growth inhibition of engineered strain (Fig. 3d). For the metal ions, the maximum voltage

291 was observed with the Zn^{2+} ion and produced high concentrations of riboflavin at pH 9 (Fig. 3e,

292 f). Concerning interference tests, the constructed MFC biosensor did not show any response to

293 Cu^{2+}, Ni^{2+}, Pb^{2+}, Hg^{2+}, and Co^{2+} metals. The constructed biosensor targeting Zn^{2+} metal ion is the

294 forefront in MFC biosensor design.

295   To monitor the toxicity in the MFC biosensor, a series of constructional and operational

296 parameters such as pH, temperature, and contaminant concentrations were considered important

297 factors which directly impact voltage generation and sensor sensitivity (Chen et al., 2016; Yi et

298 al., 2019). A good correlation between voltages and Zn^{2+} concentrations at 0–400 µM was

299 developed while increasing Zn^{2+} concentration up to 600 µM declined the voltage in the MFC

300 (Fig. 3a). The similar results were reported by Chen et al., (2016) detecting *p*-nitrophenol (PNP)

301 in wastewater has linear relations at 50 - 200 mg/L and the voltage was inhibited by increasing

302 PNP concentration to 300 mg/L. The linear correlation curve between voltages and glucose

303 concentrations (0-400 mg/L) was also observed in the MFC biosensor (Yu et al., 2017).

304 Maximum voltage and riboflavin production were observed under environmental parameters as

305 follows: Zn^{2+} concentration, 400 µM; pH 9; and temperature, 37 °C (Fig. 3).

17

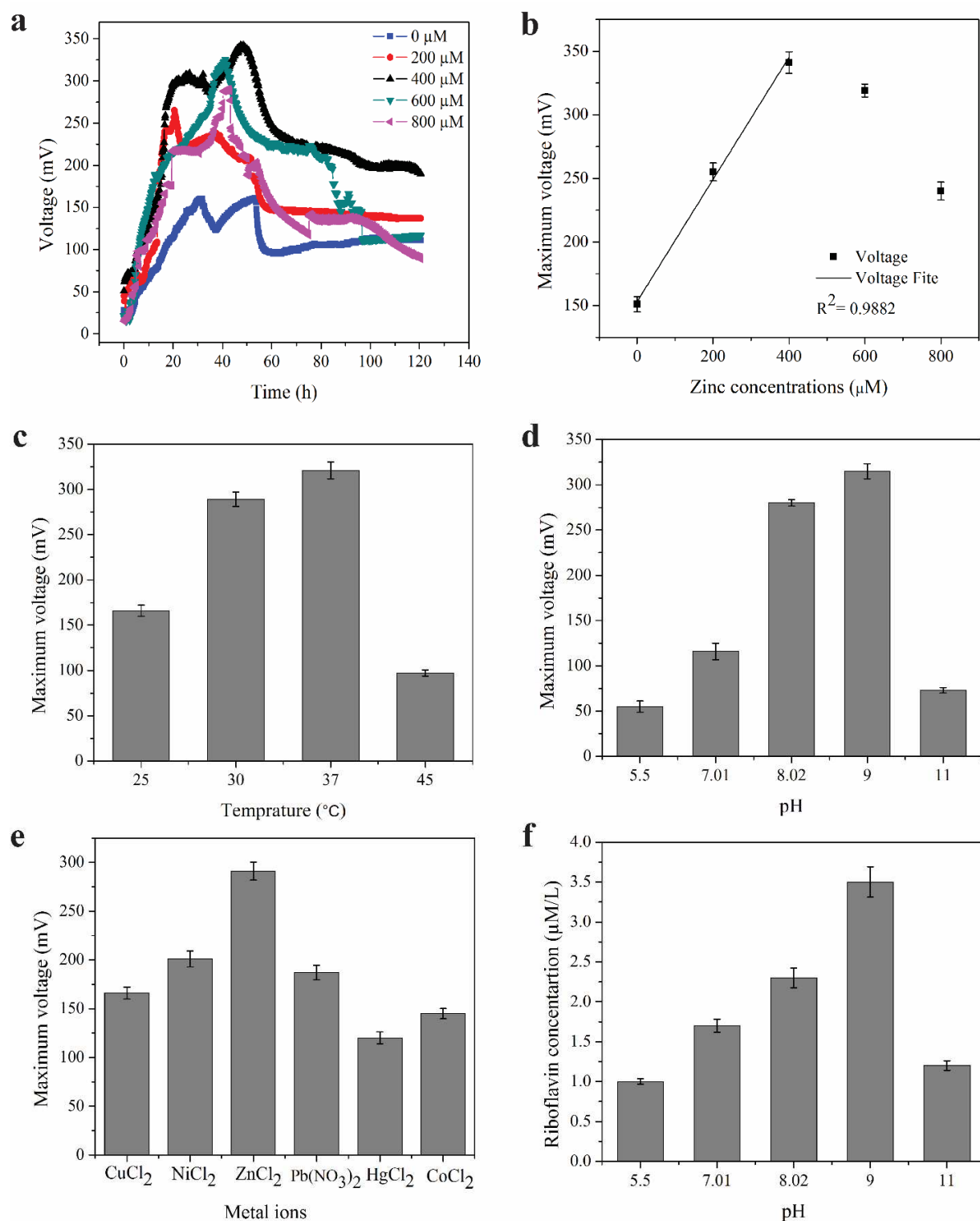**Fig. 3.** (**a**) Optimization of parameters for Zn^{2+} constructed sensor at different concentrations of Zn^{2+}, (**b**) maximum voltage output, (**c**) temperatures, (**d**) pH, (**e**) metals ions, and (**d**) riboflavin production at different pH in MFC.

18

The obtained results were in accordance with the previous reports that acidification restricted the biofilm formation, community alteration, and bacterial growth in MFCs (Patil et al., 2010; Xu et al., 2016), and alkaline pH significantly increases the synthesis of riboflavin in MFC by *S. oneidensis* MR-1 (Yong et al., 2013a; You et al., 2018). Most of the previously constructed biosensors were not specific in response to several other divalent metals. However, the Zn^{2+} specific sensor based on the reporter gene was constructed by (Liu et al., 2012), while the present biosensor is based on the MFC. This data indicated that 37 °C and pH 9 were considered as the operating temperature and pH for the detection of Zn^{2+} ranging from 0 µM to 400 µM in the constructed MFC biosensor.

3.4. Electrochemical characteristics of the constructed MFC biosensor

The maximum power density of the engineered BL21 strain reached 75 mW/m^2, which was 6.25 times higher than that of the control (12 mW/m^2). Voltage generation of the engineered BL21 strain in the open circuit was 430 mV, while the WT BL21 strain showed only 220 mV of voltage output (Fig. S1a). A pair of redox peaks of the currents by the engineered strain BL21 was much higher than that of the WT strain (Fig. S1b). In addition, SEM images confirmed that both engineered and WT BL21 strains can form biofilms on carbon felts (Fig. S1c,d). The engineered BL21 strain displayed considerable electrochemical activity in comparison to the control.

Electrochemical tensions in the MFC are related to the secretion of mediator byproducts *via* a permeable outer membrane which can promote MFC performance (Patil et al., 2010). Redox mediators work as a flexible terminal to accept and transfer electrons in the MFC (Kotloski and Gralnick, 2013), such as hydroquinone secreted by *E. coli* that can efficiently enhance the maximum power density to 1300 mW/m^2 (Qiao et al., 2008). In this study, the

329   engineered BL21 strain secreted riboflavin in anode MFC and increased cell membrane

330   permeability which increased the power density by 6.25 times as compared to the control. The

331   obtained results were consistent with that the overexpression of the *rib*ABCDE gene cluster in *S.*

332   *oneidensis* enhancing power density to 13.2 times higher than its parental strain (Yang et al.,

333   2015). *opr*F expressed in *E. coli* BL21 could significantly improve the membrane permeability

334   and power density by applying exogenous riboflavin (Yong et al., 2013b). This data suggested

335   that the engineered strain produced electroactive compounds in the MFC that promoted the

336   voltage output.

337   *3.5 MFC biosensor cross-validation with analytical methods*

338   The constructed MFC biosensor was tested by feeding the system with wastewater for

339   practical application and cross-validation with the conventional approaches. The results showed

340   that Zn^{2+} specific MFC biosensor has promising sensitivity to 0, 20, 60, and 100 µM of Zn^{2+}

341   concentrations by generating voltages of 78, 92, 146, and 201 mV, respectively (Table. S1).

342   Detection of Zn^{2+} concentrations in the wastewater was also analyzed by colorimetric, FAAS,

343   and ICP-OES methods. The results showed that there was no significant difference in the

344   determination of Zn^{2+} between analytical approaches and the MFC biosensor (Fig. 4). The Zn^{2+}

345   biosensor toward standardization in comparison with analytical methods is cost-effective, has a

346   sharp response, and a short life cycle. This data indicated that the water containing Zn^{2+}

347   monitored by the MFC-based biosensor is an economical approach.

348   Conventionally water quality monitoring by analytical approaches has a widespread use

349   with significant limitations. The conventional methods need experts to operate the equipment, is

350   often expensive, and time-consuming (Li et al., 2015), and the measured contaminant

351 concentrations of water quality do not readily reveal the definite response to humans or other
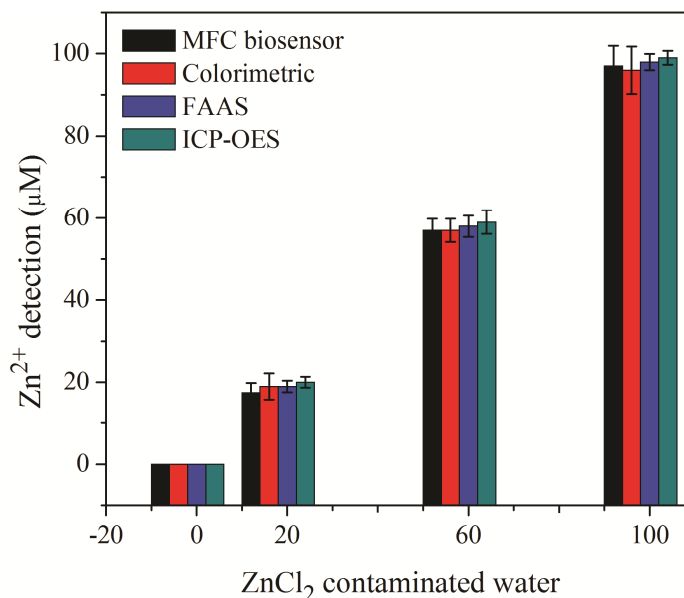
352 organisms (Jiang et al., 2018).

Fig.4. Comparison of Zn^{2+} detection in wastewater by MFC biosensor with conventional methods (Colorimetric, FAAS, and ICP-OES).

353 To address this issue, MFC biosensors function based on biological processes using

354 living organisms and could be implemented as a supplementary tool for water quality

355 assessment. An overview of Zn^{2+} detection in water by the constructed MFC biosensor in

356 comparison to that by the conventional approaches in terms of limit of detection and system cost

357 is presented in Table. 2. The MFC-based biosensors are a self-sustaining and cost-efficient

358 device for *in-situ* and online monitoring of metals in the water that avoids difficult laboratory

359 protocols and sample pre-treatment. It has the ability to interact rapidly with the toxic

360 compounds, providing a direct estimation of toxicity and has a long period of operation and less

361 maintenance compared to the analytical systems (Yu et al., 2017). Zinc ions enter into the water

362 from various sources such as pharmaceutical, agricultural, and industrial waste, which is a

363 challenging issue (Liu et al., 2019). The limited detection range of Zn^{2+} by our constructed MFC

364   biosensor was from 20 µM in water and matched the standard zinc concentrations limit in the

365   drinking water of 3 mg/L or 45.8 µM as described by the FAO and WHO, respectively (Noulas

366   et al., 2018), and 15.4 µM according to the legislation in China (Liu et al., 2012). The

367   Environmental Protection Agency (EPA) prescribed that 5 mg/L or 30 µM of zinc is toxic to the

368   environment (Ravikumar et al., 2011), was covered by our constructed MFC biosensor. This

369   approach is a new development in MFC biosensor research for monitoring of metal ions in water

370   or the aquatic environment. However, the applications of MFC biosensors are still in the early

371   stages in the detection of metals and have not been commercialized. Substantial research

372   progress has been achieved on the various aspects, including sensitivity, selectivity, real-time

373   monitoring, and cost-effectiveness while some parameters still influence the performance of

374   MFC biosensor. At present, the MFC biosensor is a cheap method developed for the detection of

375   metals compared to the conventional approaches and the potential for research toward further

376   innovation is encouraging.

Table 2

Comparison of Zn^{2+} detection by MFC biosensor with analytical methods in wastewater in cost and limited detection range.

Conventional methods	Detection principles	Sources of water	Limited detection (µM)	System setup cost ($)	References
Electrothermal atomic absorption spectroscopy (EAAS)	Atomic absorption	Irrigation water	0.0037	75k	Terres-Martos et al. (2002)
Flame atomic absorption spectroscopy (FAAS)	Atomic absorption	Runoff water	0.12	50k	(Legret and Pagotto, (1999)
Graphite furnace atomic absorption spectroscopy (GFAAF)	Atomic absorption	Seawater	0.02	75k	(Locatelli1 et al. (1999)
Inductively coupled plasma mass spectroscopy (ICP-MS)	Atomic Emission	Mineral water	.00076	100k	(Misund et al. (1999)
Inductively coupled plasma optical emission spectroscopy (ICP-OES)	Atomic Emission	Natural water	0.8	100k	(Escudero et al. (2010)
Differential plus anodic stripping voltammetry (DPASV)	Voltammetry	Sediment-water	3.52	25k	(Legret and Pagotto, (1999)
Colorimetric (Silica nanoparticles)	Fluorescence	Ground rainwater	10	1.5K	(Pham et al. (2013)
Microbial fuel cell (MFC) biosensor	Voltage	Synthetic wastewater	20	0.5k	This study

4. Conclusions

Zinc responsive regulator (p*znt*R) with *rib*B and *opr*F were collectively expressed in the *E.coli* BL21 strain and make it exoelectrogen. MFC biosensor device based on the Android App system developed by employing the engineered BL21 sensor strain revealed a high specificity to Zn^{2+} and established a good linear relationship between different Zn^{2+} concentrations and voltages output. The constructed MFC biosensor detected 20 μM of Zn^{2+} in water which covers the safety standard of Zn^{2+} in drinking water. It is self-powered, affordable, and is an alternative to conventional methods for the detection of metals in water. This MFC-based biosensor is the first Zn^{2+} biosensor of its kind and future applications need to be explored.

Appendix A. Supporting information

Supplementary data associated with this article can be found in the online version at

References

Arcidiacono, S., Soares, J.W., Meehan, A.M., Marek, P., Kirby, R., 2009. J. Pept. Sci. 15(6), 398-403.

Bereza-Malcolm, L.T., Mann, G., Franks, A.E., 2015. ACS synth. bio. 4(5), 535-546.

Catal, T., Kul, A., Atalay, V.E., Bermek, H., Ozilhan, S., Tarhan, N., 2019. J. of P. Sour. 414, 1-7.

Cerminati, S., Soncini, F.C., Checa, S.K., 2011. Biotech. and bioeng. 108(11), 2553-2560.

Cerminati, S., Soncini, F.C., Checa, S.K., 2015. Chemical communications 51(27), 5917-5920.

404 Chen, Z., Niu, Y., Zhao, S., Khan, A., Ling, Z., Chen, Y., Liu, P., Li, X., 2016. Biosen.
405   Bioelectron. 85, 860-868.
406 Choi, S.H., Lee, K.L., Shin, J.H., Cho, Y.B., Cha, S.S., Roe, J.H., 2017. Nat Commun. 8, 15812.
407 Escudero, L.A., Martinez, L.D., Salonia, J.A., Gasquez, J.A., 2010. Micro. J. 95(2), 164-168.
408 Ivask, A., Virta, M., Kahru, A., 2002. Soil bio. & biochem. 34(10), 1439-1447.
409 Jiang, Y., Yang, X., Liang, P., Liu, P., Huang, X., 2018. Rene. and Sust. En. Rev. 81, 292-305.
410 Kim, H.J., Lim, J.W., Jeong, H., Lee, S.J., Lee, D.W., Kim, T., Lee, S.J., 2016. Biosen.
411   Bioelectron. 79, 701-708.
412 Kim, M., Sik Hyun, M., Gadd, G.M., Joo Kim, H., 2007. J Environ Monit 9(12), 1323-1328.
413 Kotloski, N.J., Gralnick, J.A., 2013. MBio 4(1).
414 Legret, M., Pagotto, C., 1999. Sci Total Environ 235(1-3), 143-150.
415 Li, L., Liang, J., Hong, W., Zhao, Y., Sun, S., Yang, X., Xu, A., Hang, H., Wu, L., Chen, S.,
416   2015. Enviro. sci. technol. 49(10), 6149-6155.
417 Li, M., Zhou, M., Tian, X., Tan, C., McDaniel, C.T., Hassett, D.J., Gu, T., 2018. Biot. adv.
418   36(4), 1316-1327.
419 Liu, P., Huang, Q., Chen, W., 2012. Environ Pollut 164, 66-72.
420 Liu, Y., Wang, Z., Liu, J., Levar, C., Edwards, M.J., Babauta, J.T., Kennedy, D.W., Shi, Z.,
421   Beyenal, H., Bond, D.R., Clarke, T.A., Butt, J.N., Richardson, D.J., Rosso, K.M., Zachara,
422   J.M., Fredrickson, J.K., Shi, L., 2014. Environ Microbiol Rep 6(6), 776-785.
423 Liu, Z., Chen, B., Li, X., Wang, L.A., Xiao, H., Liu, D., 2019. Sci Total Environ 670, 433-438.
424 Locatelli1, C., Astara, A., Vasca, E., Campanella, V., 1999. Enviro. monitor. and asses. 58(23–
425   37).
426 Logan, B.E., 2009. Nat Rev Microbiol 7(5), 375-381.
427 Misund, A., Frengstad, B., Siewers, U., Reimann, C., 1999. Sci Total Environ 243-244, 21-41.
428 Muheim, C., Gotzke, H., Eriksson, A.U., Lindberg, S., Lauritsen, I., Norholm, M.H.H., Daley,
429   D.O., 2017. Sci. rep. 7(1), 17629.
430 Noulas, C., Tziouvalekas, M., Karyotis, T., 2018. J Trace Elem Med Biol 49, 252-260.
431 Patil, S.A., Harnisch, F., Kapadnis, B., Schroder, U., 2010. Biosens. Bioelectron. 26(2), 803-808.
432 Peca, L., Kos, P.B., Mate, Z., Farsang, A., Vass, I., 2008. FEMS microbio. lett. 289(2), 258-264.
433 Pham, V.D., Ravikumar, S., Lee, S.H., Hong, S.H., Yoo, I.K., 2013. Biopro. Biosyst Eng 36(9),
434   1185-1190.
435 Poddalgoda, D., Macey, K., Hancock, S., 2019. Regul Toxicol Pharmacol.
436 Qiao, Y., Li, C.M., Bao, S.J., Lu, Z., Hong, Y., 2008. Chem. comm. (11), 1290-1292.
437 Ravikumar, S., Ganesh, I., Yoo, I.-k., Hong, S.H., 2012. Pro. Biochemistry 47(5), 758-765.
438 Ravikumar, S., Yoo, I.K., Lee, S.Y., Hong, S.H., 2011. Biop. Biosyst Eng 34(9), 1119-1126.
439 Rijavec, T., Zrimec, J., Oven, F., Viršek, M.K., Somrak, M., Podlesek, Z., Gostinčar, C.,
440   Leedjärv, A., Virta, M., Tratnik, J.S., Horvat, M., Lapanje, A., 2016. Geomicrobiology J.
441   34(7), 596-605.
442 Su, L., Jia, W., Hou, C., Lei, Y., 2011. Biosens. & bioelectron. 26(5), 1788-1799.
443 Takeuchi, A., Namera, A., Sakui, N., Yamamoto, S., Yamamuro, K., Nishinoiri, O., Endo, Y.,
444   Endo, G., 2019. J Occup Health 61(1), 82-90.
445 Tanikkul, P., Pisutpaisal, N., 2018. Int. J. of Hydr.En. 43(1), 483-489.
446 Tao, L., Wang, H., Xie, M., Thia, L., Chen, W.N., Wang, X., 2015. Chem. commun. 51(61),
447   12170-12173.
448 Terres-Martos, C., Navarro-Alarcon, M., Martin-Lagos, F., Gimenez-Martinez, R., Lopez-Garcia
449   De La Serrana, H., Lopez-Martinez, M.C., 2002. Water res. 36(7), 1912-1916.

450 Vasilaki, A.T., McMillan, D.C., Kinsella, J., Duncan, A., O'Reilly, D.S., Talwar, D., 2010. Clin
451   Chim Acta 411(21-22), 1750-1755.

452 Watstein, D.M., Styczynski, M.P., 2018. ACS synth. bio.7(1), 267-275.

453 Webster, D.P., TerAvest, M.A., Doud, D.F., Chakravorty, A., Holmes, E.C., Radens, C.M.,
454   Sureka, S., Gralnick, J.A., Angenent, L.T., 2014. Biosen. Bioelectron. 62, 320-324.

455 Wen, Q., Kong, F., Ma, F., Ren, Y., Pan, Z., 2011. J. of P. Sour.196(3), 899-904.

456 Xu, Y.S., Zheng, T., Yong, X.Y., Zhai, D.D., Si, R.W., Li, B., Yu, Y.Y., Yong, Y.C., 2016.
457   Bioresou. technol. 211, 542-547.

458 Yang, Y., Ding, Y., Hu, Y., Cao, B., Rice, S.A., Kjelleberg, S., Song, H., 2015. ACS synthetic
459   biology 4(7), 815-823.

460 Yi, Y., Xie, B., Zhao, T., Li, Z., Stom, D., Liu, H., 2019. Bioelectrochemistry 125, 71-78.

461 Yi, Y., Xie, B., Zhao, T., Liu, H., 2018. Bioresou. technol. 265, 415-421.

462 Yong, X.Y., Shi, D.Y., Chen, Y.L., Feng, J., Xu, L., Zhou, J., Wang, S.Y., Yong, Y.C., Sun,
463   Y.M., OuYang, P.K., Zheng, T., 2014. Bioresou. technol. 152, 220-224.

464 Yong, Y.C., Cai, Z., Yu, Y.Y., Chen, P., Jiang, R., Cao, B., Sun, J.Z., Wang, J.Y., Song, H.,
465   2013a. Bioresou. technol. 130, 763-768.

466 Yong, Y.C., Yu, Y.Y., Yang, Y., Liu, J., Wang, J.Y., Song, H., 2013b. Biotech. and bioeng.
467   110(2), 408-416.

468 You, L.X., Liu, L.D., Xiao, Y., Dai, Y.F., Chen, B.L., Jiang, Y.X., Zhao, F., 2018.
469   Bioelectrochemistry 119, 196-202.

470 Yu, D., Bai, L., Zhai, J., Wang, Y., Dong, S., 2017. Talanta 168, 210-216.

471 Yu, D., Zhai, J., Yong, D., Dong, S., 2013. Analyst 138(11), 3297-3302.

472

Highlights

- Engineered *E.coli* strain co-expresses p*znt*R, *rib*B, and *opr*F in MFC system.

- Linear relationship is established between Zn^{2+} concentration and voltage.

- Constructed MFC biosensor detects Zn^{2+} in the range of 20-400 µM/L.

- Zn^{2+} detection by MFC biosensor is consistent with conventional approaches.

CRediT author statement

A.K., E.S.S. and X.K.L: Conceptualization; Methodology; Data Curation; Investigation; Formal analysis; Review & editing.

A.K. and H.N: Original draft writing

A.K., Z.C., S.Z. and T.Z: Software development; Data Curation

P.Y., R.K.S. and Z. L: Review & editing.

X.K.L., P.L and E.S.S: Funding acquisition; Project administration; Supervision

Declaration of interest statement

Date, 26th July 2019

We confirm that the manuscript entitled "A novel biosensor for zinc detection based on microbial fuel cell system" has been read and approved by all named authors. The authors declare that they have no known competing financial interests or personal relationships that could have appeared to influence the work reported in this paper.

We understand that the *Corresponding Author* is the sole contact for the Editorial process (including Editorial Manager and direct communications with the office). He is responsible for communicating with the other authors about progress, submissions of revisions and final approval of proofs. We confirm that we have provided a current, correct email address which is accessible by the *corresponding Author*.

Sincerely yours,

Xiangkai Li Ph. D. (*Corresponding Author*)

School of Life Sciences, Lanzhou University,

Lanzhou, Gansu, 730000, P. R. China,

Tel: 86-931-8912561,

Fax: 86-931-8912560,

E-mail: xkli@lzu.edu.cn